



iJRASET

International Journal For Research in
Applied Science and Engineering Technology



INTERNATIONAL JOURNAL FOR RESEARCH

IN APPLIED SCIENCE & ENGINEERING TECHNOLOGY

Volume: 3

Issue: V

Month of publication: May 2015

DOI:

www.ijraset.com

Call:  08813907089

E-mail ID: ijraset@gmail.com

D-STATCOM Based Multi-Level Inverter for Reactive Power Compensation

Srinivasa Acharya¹, B. Trinadha², B. Srinivasa Rao³

^{1,2}Assistant professor, ³Associate professor

Dept. of EEE, Aditya Institute Of Technology And Management, Tekkali, Srikakulam (Dist), A.P., India

ABSTRACT-The line upgrading techniques with Static Synchronous Compensator (STATCOM) is one of the promising technologies applied to improve power system performance. The STATCOMs in the distribution utilities (DSTATCOMs) are increasingly investigated for dynamic reactive power compensation and power quality improvement in the distribution utilities. This paper presents an investigation of seven-Level Cascaded H - bridge (CHB) Inverter as Distribution Static Compensator (DSTATCOM) in Power System (PS) for compensation of reactive power and harmonics. The simplification and analyzing of three phase circuits can be done by d-q reference frame theory. The DST ATCOM helps to improve the power factor and eliminate the Total Harmonics Distortion (THD) drawn from a Non- Liner Diode Rectifier Load (NLDRL). Finally a level shifted PWM (LSPWM) and phase shifted PWM (PSPWM) techniques are adopted to investigate the performance of CHB Inverter. The results are obtained through Matlab / Simulink software package.

Keywords: DSTATCOM, Cascaded H bridge (CHB), proportional integral (PI) control, D-Q reference frame theory.

I. INTRODUCTION

Multilevel inverters are mainly utilized to synthesis a desired single- or three-phase voltage waveform. The desired multi-staircase output voltage is obtained by combining several dc voltage sources. Solar cells, fuel cells, batteries and ultra-capacitors are the most common independent sources used[1]. One important application of multilevel converters is focused on medium and high-power conversion. Nowadays, there exist three commercial topologies of multilevel voltage-source inverters: neutral point clamped (NPC), cascaded H-bridge (CHB), and flying capacitors (FCs)[3]. Among these inverter topologies, cascaded multilevel inverter reaches the higher output voltage and power levels (13.8 kV, 30 MVA) and the higher reliability due to its modular topology[4]. Multilevel power conversion has become increasingly popular in recent years due to advantages of high power quality waveforms, low electromagnetic compatibility (EMC) concerns, low switching losses, and high-voltage capability [2]–[5]. The primary disadvantage of this technology is the large number of semiconductor devices required. This does not yield a significant cost increase since lower-voltage devices may be used. However, an increase in gate drive circuitry and more elaborate mechanical layout are required. Although the diode clamped multilevel inverter [2]–[5] is commonly discussed in the literature, there has been considerable interest in the series connected or cascaded H-bridge inverter topologies [8]–[25]. The primary advantage of this structure is its simplicity and that fewer or more H-bridge cells can be cascaded in order to decrease or increase the voltage and power level respectively. The main disadvantage of this topology is that each H-bridge cell requires an isolated dc source. The isolated sources are typically provided from a transformer/rectifier arrangement [6], but may be supplied from batteries, capacitors [8] or photovoltaic arrays [18]. Recent advances in cascaded H-bridge inverters include utilizing different dc voltages on each series H-bridge in order to increase the number of voltage levels and improve the power quality [19]–[23]. In other research, two five-level H-bridge cells, operating at the same dc voltage, were cascaded forming a novel type of inverter [24] which can operate as a nine-level inverter. In this paper, the general idea of cascading multilevel H-bridge cells is introduced. This differs from previous research [19]–[24] in that there may be any number of cells, each with an arbitrary number of levels, and each with a unique dc voltage value in order to maximize power quality. This new topology will be referred to as a cascaded multilevel H-bridge inverter. This paper contains generalized mathematical equations for determining the dc voltage ratio required in order to maximize power quality based on the number of multilevel cells. The STATCOM used in distribution systems is called DSTACOM (Distribution-STACOM) and its configuration is the same, but with small modifications. It can exchange both active and reactive power with the distribution system by varying the amplitude and phase angle of the converter voltage with respect to the line terminal voltage. A multilevel inverter can reduce the device voltage and the output harmonics by increasing the number of output voltage levels. There are several types of multilevel inverters: cascaded R-bridge (CRB), neutral point clamped, flying capacitor [2-5]. In particular, among these topologies, CRB

International Journal for Research in Applied Science & Engineering Technology (IJRASET)

inverters are being widely used because of their modularity and simplicity. Various modulation methods can be applied to CRB inverters. CRB inverters can also increase the number of output voltage levels easily by increasing the number of R-bridges. This paper presents a DSTATCOM with a proportional integral controller based CRB multilevel inverter for the harmonics and reactive power mitigation of the nonlinear loads. This type of arrangements have been widely used for PQ applications due to increase in the number of voltage levels, low switching losses, low electromagnetic compatibility for hybrid filters and higher order harmonic elimination.

A. Static Synchronous Compensator

Static Synchronous Compensator (STATCOM) is a voltage source converter based FACTS controller. It is a shunt controller mainly used to regulate voltage by generating/absorbing reactive power. The schematic diagram of STATCOM is shown in Fig. 1. STATCOM has no long term energy support in the DC Side and cannot exchange real power with the ac system ; however it can exchange reactive power. The reactive power is varied by varying the magnitude of the converter output voltage. A small phase difference exists between the converter output voltage and STATCOM bus voltage so that real power is drawn from the lines to compensate for the losses. STATCOMs are employed at distribution and transmission levels – though for different purposes.

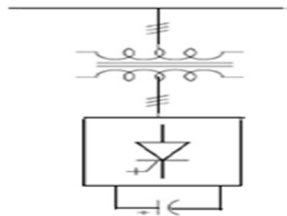


Fig.1. schematic diagram of STATCOM

B. Voltage Source Converters

In recent years, voltage source converter technology has made a great progress through the development of high power self-turnoff type semiconductor devices. The rating for converter of this type in practical application has already reached as high.

Because of its advantage over the line commutated type in performance characteristics and compactness, various applications of the voltage source converter have been developed and researched. Three phase Voltage Source Converter (VSC) is heart of most new FACTS and custom power equipments. It may be employed as a series or shunt element or combination of both, as in case of Unified Power Flow Controller (UPFC). Multilevel Voltage Source Converter topology is superior alternative to multipulse arrangement for high power applications like STATCOM. Voltage source converters (VSC) are commonly used to transfer power between a dc system and an ac system or back to back connection for ac systems with different frequencies, such as variable speed wind turbine systems[2]. A basic VSC structure is shown in Fig. 2 where R_s and L_s represent the resistance and inductance between the converter ac voltage (V_c) and the ac system voltage (V_s) and I_s is the current injected into the grid. A dc capacitor is connected on the dc side to produce a smooth dc voltage. The switches in the circuit represent controllable semiconductors, such as IGBT or power transistors. 6-pulse D-STATCOM configuration with the IGBT's used as power devices. The IGBTs are connected anti parallel with diodes for commutation purposes and charging of the DC capacitor. For converter the most important part is the sequences of operation of the IGBTs. The IGBTs signals are referred to the Pulse Width Modulation (PWM) that will generate the pulses for the firing of the IGBTs. IGBTs are used in this simulation because it is easy to control the switch on and off of their gates and suitable for the D-STATCOM.

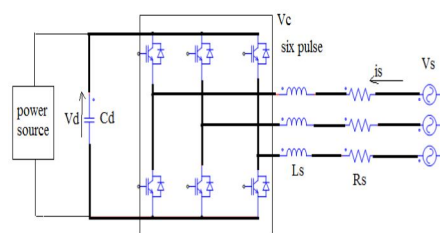


Fig. 2 Voltage source converter (V_{sc})

International Journal for Research in Applied Science & Engineering Technology (IJRASET)

C. Basic Configuration and Operation Of DSTATCOM

When a STATCOM is employed at the distribution level or at the load end for power factor improvement and voltage regulation alone it is called D-STATCOM. Fig.2 shows a basic configuration diagram of the D-STATCOM. The D-STATCOM mainly consists of DC voltage source behind self-commutated inverters using IGBT and coupling transformer. The IGBT inverter with a DC voltage source can be modeled as a variable voltage source. The distribution power system can also be modeled as a voltage source. Two voltage sources are connected by a

$$I = (V - V_o) / X \quad (1)$$

Reactor representing the leakage reactance of the transformer. The principle operation modes of the D-STATCOM output current, I which varies depending upon the voltage. Where V , V_o , X are the system voltage, output voltage of the IGBT-based inverter, the total ckt reactance respectively. If V_o is equal to V , then no reactive power is delivered to the system. If V_o is greater than V , the phase angle of I is leading with respect to the phase angle of V by 90 degrees. Thus, a leading reactive power flows in the Capacitive Mode of the D-STATCOM. If V_o is lower than V , the phase angle of I is lagging with respect to the phase angle of V by 90 degrees. Thus, a lagging reactive power flows in the Inductive Mode of the D-STATCOM.

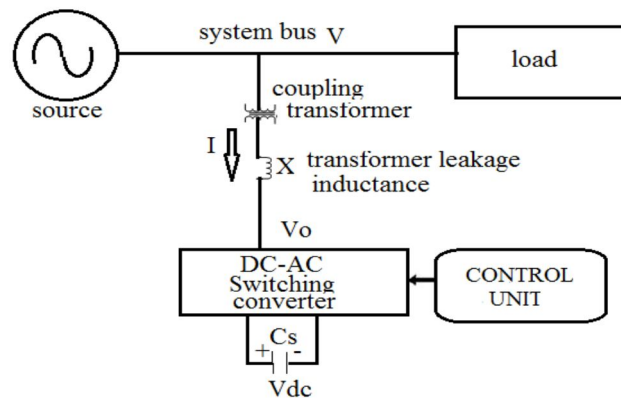


Fig.3.Single-line diagram of D-STATCOM

II. H-BRIDGE MULTILEVEL INVERTER

The traditional two or three levels inverter does not completely eliminate the unwanted harmonics in the output waveform. Therefore, using the multilevel inverter as an alternative to traditional PWM inverters is investigated. In this topology the number of phase voltage levels at the converter terminals is $2N+1$, where N is the number of cells or dc link voltages. In this topology, each cell has separate dc link capacitor and the voltage across the capacitor might differ among the cells. So, each power circuit needs just one dc voltage source. The number of dc link capacitors is proportional to the number of phase voltage levels. Each H-bridge cell may have positive, negative or zero voltage. Final output voltage is the sum of all H-bridge cell voltages and is symmetric with respect to neutral point, so the number of voltage levels is odd. Cascaded H-bridge multilevel inverters typically use IGBT switches. These switches have low block voltage and high switching frequency. Fig.4.

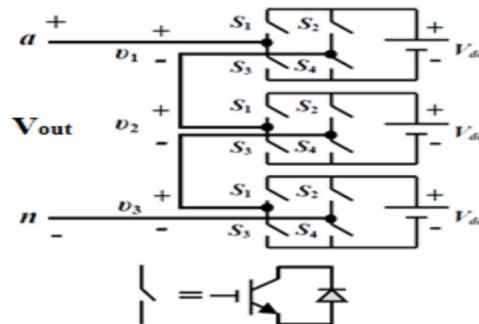


Fig 4. Cascaded H-bridge 7-level Inverter

International Journal for Research in Applied Science & Engineering Technology (IJRASET)

Consider the seven level inverter; it requires 12 IGBT switches and three dc sources. The power circuit of inverter is shown in the figure 4. A cascaded H-bridges multilevel inverter is simply a series connection of multiple Hbridge inverters. Each H-bridge inverter has the same configuration as a typical single-phase full-bridge inverter.

The cascaded H-bridges multilevel inverter introduces the idea of using Separate DC Sources (SDCSs) to produce an AC voltage waveform. Each H-bridge inverter is connected to its own DC source V_{dc} . By cascading the AC outputs of each H-bridge inverter, an AC voltage waveform is produced.

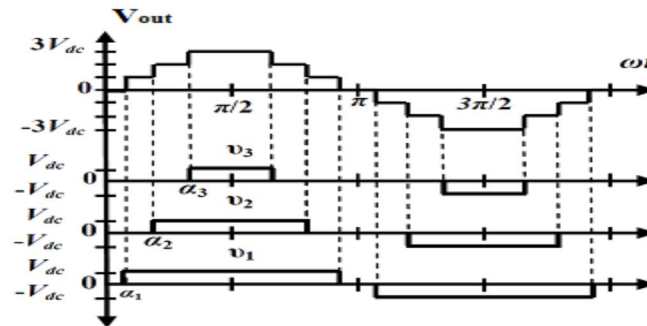


Fig 5. Output Voltage of cascaded H-bridge seven level inverter

By closing the appropriate switches, each H-bridge inverter can produce three different voltages: $+V_{dc}$, 0 and $-V_{dc}$. It is also possible to modularize circuit layout and packaging because each level has the same structure, and there are no extra clamping diodes or voltage balancing capacitors. The number of switches is reduced using the new topology. This circuit is simulated using the MATLAB software. The results are shown in the later sections in detail.

III. PROPOSED TOPOLOGY

The main objective is to improve the quality output voltage of the multilevel inverter with reduced number of switches. An important

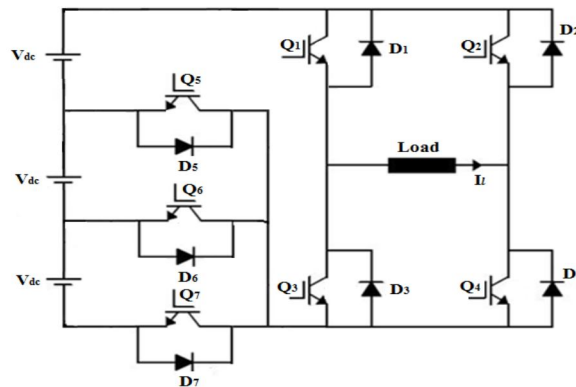


Fig.6. Proposed Power circuit for 7-level output

issue in multilevel inverter design is that to generate nearly sinusoidal output voltage waveform and to eliminate lower order harmonics. A key concern in the fundamental switching scheme is to determine the switching angles in order to produce the voltage with fundamental frequency. There are three modes of operation for the proposed 7-level multilevel inverter. These modes are explained as below.

A. Powering Mode

This occurs when both the load current and voltage have the same polarity. In the positive half cycle, when the output voltage is V_{dc} , the current pass comprises; the lower supply, D_6 , Q_1 , load, Q_4 , and back to the lower supply. When the output voltage is

International Journal for Research in Applied Science & Engineering Technology (IJRASET)

2Vdc, current pass is; the lower source, Q5, the upper source, Q1, load, Q4, and back to the lower source. When the output voltage is 3Vdc, the current pass comprises: upper supply, Q1, load, Q4, Q7, lower supply. In the negative half cycle, Q1 and Q4 are replaced by Q2 and Q3 respectively.

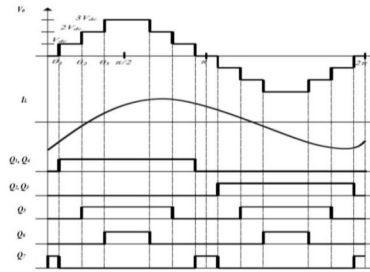


Fig.7. Waveforms of the proposed seven level inverter

B. Free-Wheeling Mode

Free-wheeling modes exist when one of the main switches is turned-off while the load current needs to continue its pass due to load inductance. This is achieved with the help of the anti-parallel diodes of the switches, and the load circuit is disconnected from the source terminals. In this mode, the positive half cycle current pass comprises; Q1, load, and D2 or Q4, load, and D3, while in the negative half cycle the current pass includes Q3, load, and D4 or Q2, load, and D1.

C. Regenerating Mode

In this mode, part of the energy stored in the load inductance is returned back to the source. This happens during the intervals when the load current is negative during the positive half cycle and viceversa, where the output voltage is zero. The positive current pass comprises; load, D2, Q6, the lower source, and D3, while the negative current pass comprises; load, D1, Q6, the lower source, and D4.

From the figure 7 switching pattern for the various switches are explained. In this paper fundamental frequency switching scheme is employed which reduces the switching losses. Because the switching frequency is less in this method when compared to the other methods. Switching losses are directly proportional to the switching frequency.

IV. DESIGN OF SINGLE H-BRIDGE CELL

A. Device Current

The IGBT and DIODE currents can be obtained from the load current by multiplying with the corresponding duty cycles. Duty cycle, $d = \frac{1}{2} (1 + K_m \sin \omega t)$ Where, m = modulation index $K = +1$ for IGBT, -1 for Diode. For a load current given by

$$i_{\text{device}} = \sqrt{2} I \sin(\omega t - \Phi) \quad (2)$$

The average value of the device current over a cycle is calculated as

$$\begin{aligned} i_{\text{device}} &= \int_{\Phi}^{\pi+\Phi} \frac{\sqrt{2}}{2} I \sin(\omega t - \Phi) \times (1 + K_m \sin \omega t) d\omega t \\ &= \sqrt{2} I \left[\frac{1}{2\pi} + \frac{K_m}{g} \cos \Phi \right] \quad (3) \end{aligned}$$

The device RMS current can be written as

$$i_{\text{rms}} = \sqrt{\int_{\Phi}^{\pi+\Phi} \frac{1}{2\pi} \left(\sqrt{2} I \sin(\omega t - \Phi) \right)^2 \times \frac{1}{2} (1 + K_m \sin \omega t) d\omega t}$$

International Journal for Research in Applied Science & Engineering Technology (IJRASET)

$$= \sqrt{2}I \sqrt{\frac{1}{g} + \frac{K_m}{3\Pi} \cos\Phi} \quad (4)$$

B. IGBT Loss Calculation

IGBT loss can be calculated by the sum of switching loss and conduction loss. The conduction loss can be calculated by,

$P_{on}(\text{IGBT}) =$

$$V_{ce0} * I_{avg(igbt)} + I_{rms(igbt)}^2 * r_{ce0} \quad (5)$$

$$I_{avg(igbt)} = \sqrt{2} I \left[\frac{1}{2\Pi} + \frac{m}{g} \cos\Phi \right] \quad (6)$$

$$I_{rms(igbt)} = \sqrt{2} I \sqrt{\left[\frac{1}{g} + \frac{m}{3\Pi} \cos\Phi \right]} \quad (7)$$

Values of V_{ce0} and r_{ce0} at any junction

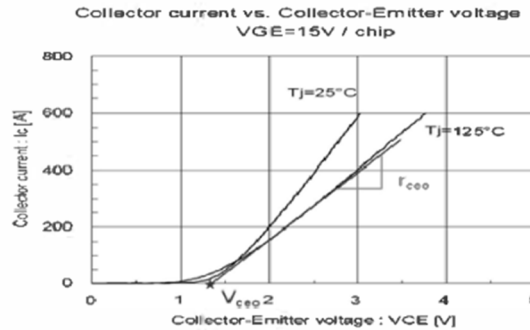


Fig. 8 IGBT output characteristics

temperature can be obtained from the output characteristics (I_c vs. V_{ce}) of the IGBT as shown in Figure-8.

The switching losses are the sum of all turn-on and turn-off energies at the switching events

$$E_{sw} = E_{on} + E_{off} = a + bI + cI^2 \quad (8)$$

Here V_{DC} is the actual DC-Link voltage and V_{nom} is the DC Link Voltage at which E_{sw} is given. Switching losses are calculated by summing up the switching energies

$$P_{sw} = \frac{1}{T_0} \sum_n E_{sw}(i) \quad (9)$$

Here 'n' depends on the switching frequency

$$P_{sw} = \frac{1}{T_0} \sum_n (a + bI + cI^2) \\ = \frac{1}{T_0} \left[\frac{a^-}{2} + \frac{bI^-}{\Pi} + \frac{cI^{2^-}}{4} \right] \quad (10)$$

After considering the DC-Link voltage variations, switching losses of the IGBT can be written as follows.

International Journal for Research in Applied Science & Engineering Technology (IJRASET)

$$P_{sw(IGBT)} = f_{sw} \left[\frac{a}{2} + \frac{bI}{\Pi} + \frac{cI^2}{4} \right] * \frac{V_{DC}}{V_{nor}} \quad (11)$$

So, the sum of conduction and switching losses is the total losses given by

$$P_{T(IGBT)} = P_{on(IGBT)} + P_{sw(IGBT)} \quad (12)$$

C. Diode Loss Calculation

The DIODE switching losses consist of its reverse recovery losses; the turn-on losses are negligible.

$$E_{rec} = a + bI + cI^2 \quad (13)$$

$$P_{sw(DIODE)} = P_{on(DIODE)} + P_{sw(DIODE)} \quad (14)$$

So, the sum of conduction and switching losses gives the total DIODE losses.

$$P_{T(DIODE)} = P_{on(DIODE)} + P_{sw(DIODE)} \quad (15)$$

The total loss per one switch (IGBT + DIODE) is the sum of one IGBT and DIODE loss.

$$P_T = P_{T(IGBT)} + P_{T(DIODE)} \quad (16)$$

D. Thermal Calculations

The junction temperatures of the IGBT and DIODE are calculated based on the device power losses and thermal resistances. The thermal resistance equivalent circuit for a module is shown in Fig 5. In this design the thermal calculations are started with heat sink temperature as the reference temperature. So, the case temperature from the model can be written as follows.

$$T_C = P_T R_{th(c-h)} + T_h \quad (17)$$

Here $R_{th(c-h)}$ = Thermal resistance between case and heatsink

$$P_T = \text{Total Power Loss (IGBT + DIODE)} \quad (18)$$

IGBT junction temperature is the sum of the case temperature and temperature raise due to the power losses in the IGBT.

$$T_{j(DIODE)} = P_{T(DIODE)} + R_{th(j-c)DIODE} + T_C \quad (19)$$

The above calculations are done based on the average power losses computed over a cycle. So, the corresponding thermal calculation gives the average junction temperature. In order to make the calculated values close to the actual

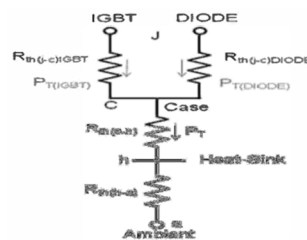


Fig. 9 Thermal resistance equivalent circuit

values, transient temperature values are to be added to the average junction temperatures.

E. DC-Capacitor Selection

The required capacitance for each cell depends on the allowable ripple voltage and the load current. The rms ripple current flowing into the capacitor can be written as follows and the ripple current frequency is double the load current frequency.

International Journal for Research in Applied Science & Engineering Technology (IJRASET)

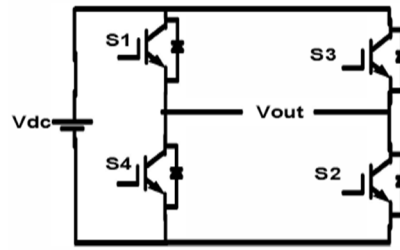


Fig.10 H-Bridge converter

$$I_c = -\frac{1}{V_{dc}} \frac{1}{2} \left(|U_{ac}| * K + I_{WL} \right) \sin(2\omega t) \quad (20)$$

Since the value of 'L' is very small, the above equation can be simplified to

$$I_c = -\frac{1}{V_{dc}} \frac{1}{2} \left(|U_{ac}| * K \right) \sin(2\omega t) \quad (21)$$

$$\begin{aligned} I_c &= -K \frac{1}{2} \frac{|U_{ac}|}{V_{dc}} * \sin(2\omega t) \\ &= -K \frac{m}{2} \sin(2\omega t) \end{aligned} \quad (22)$$

Here 'm' is the modulation index and

$$\begin{aligned} I_{cp} &= C \frac{du_{pp}}{dt} ; \sin(2\omega t) \\ &= \frac{m}{2} I \sqrt{2} = C 2\omega * \Delta V V_{dc} \end{aligned} \quad (23)$$

$$C = \frac{m}{4\omega} \frac{1}{\Delta V * V_{dc}} \sqrt{2} I \quad (24)$$

F. PWM Techniques For CHB Inverter

The most popular PWM techniques for CHB inverter are 1. Phase Shifted Carrier PWM (PSCPWM), 2. Level Shifted Carrier PWM (LSCPWM).

1) Phase Shifted Carrier PWM (PSCPWM):

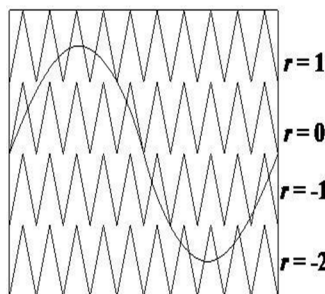


Fig.11 Phase Shifted Carrier PWM

Figure-11 shows the Phase shifted carrier pulse width modulation. Each cell is modulated independently using sinusoidal unipolar pulse width modulation and bipolar pulse width modulation respectively, providing an even power distribution among the cells. A

International Journal for Research in Applied Science & Engineering Technology (IJRASET)

carrier phase shift of $180^\circ / m$ (No. of levels) for cascaded inverter 1S introduced across the cells to generate the stepped multi level output waveform with lower distortion.

2. *Level Shifted Carrier PWM (LSCPWM)*: Figure-12 shows the Level shifted carrier pulse width modulation. Each cell is modulated independently using sinusoidal unipolar width modulation and bipolar pulse width modulation respectively, providing an even power distribution among the cells. A carrier Level shift by $1/m$ (No.

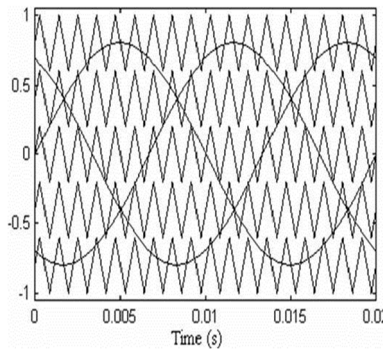


Fig.12 Level Shifted Carrier PWM

of levels) for cascaded inverter 1S introduced across the cells to generate the stepped multilevel output waveform with lower distortion.

IV. MATLAB/SIMULINK MODELING AND SIMULATION RESULTS

Figure- 13 shows the Matab/Simulink power circuit model of DSTATCOM. It consists of five blocks named as source block, non linear load block, control block, APF block and measurements block. The system parameters for simulation study are source voltage of 11kv, 50 hz AC supply, DC bus capacitance 1550 e-6 F, Inverter series inductance 10 mH, Source resistance of 0.1 ohm and inductance of 0.9 mh. Load resistance and inductance are chosen as 30mh and 60 ohms respectively.

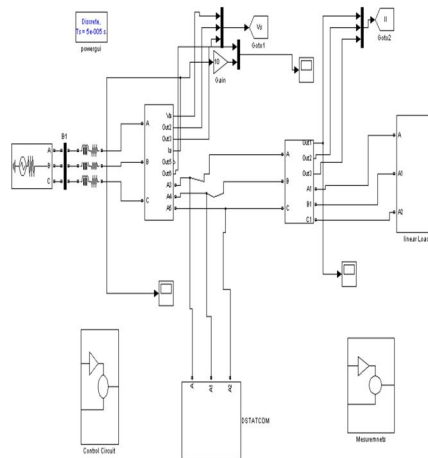


Fig. 13 Matlab/Simulink power circuit model of DSTATCOM

Figure-14 shows the phase- A voltage of seven level output of phase shifted carrier PWM inverter.

International Journal for Research in Applied Science & Engineering Technology (IJRASET)

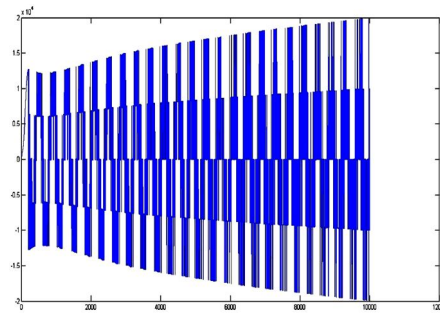


Fig. 14seven level PSCPWM output

Figure-15, 16, 17 shows the three phase source voltages, three phase source currents and load currents respectively without DST AT COM. It is clear that without DSTAT COM load current and source currents are same.

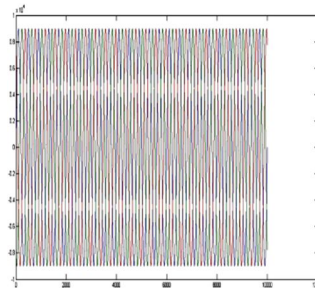


Fig. 15 Three phase source voltage versus time

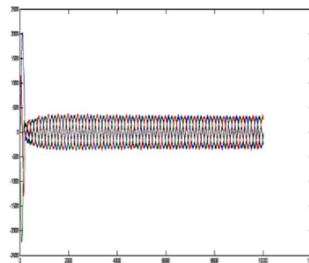


Fig. 16 Three phase source current versus time

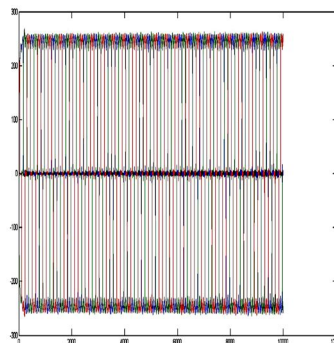


Fig. 17 Load current versus time

International Journal for Research in Applied Science & Engineering Technology (IJRASET)

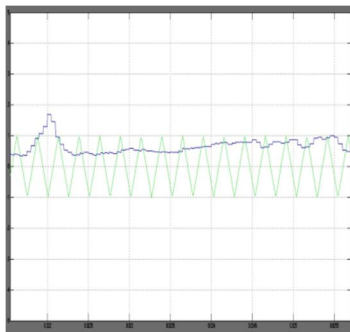


Figure 18 indicates the phase voltage and currents by applying different load conditions.

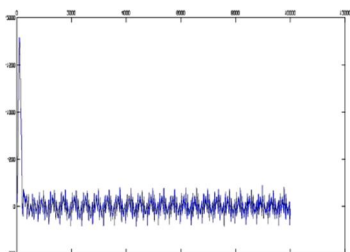


Fig. 18 Phase A source voltage and current

Figure 19, 20 indicates controller fluctuations on both input and output sides. By using DSTATCOM the fluctuations are minimized in a less number.

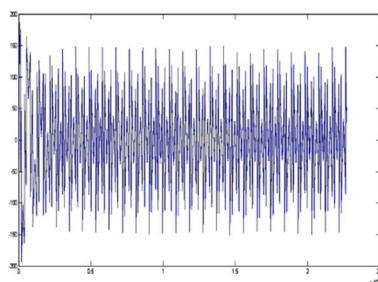


Fig. 19 Controller input voltage fluctuations

Fig. 20 Controller output voltage fluctuations

Figure-21 shows the harmonic spectrum of Phase - A Source current without DST ATCOM. The THD of source current without DST ACOM is 31.31%.

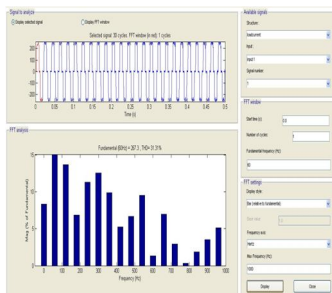


Fig. 21 Harmonic spectrum of Phase-A Source current without DSTATCOM

Figure-22 shows the harmonic spectrum of Phase - A Source current with DST ATCOM. The THD of source current without DST ACOM is 9.75%

International Journal for Research in Applied Science & Engineering Technology (IJRASET)

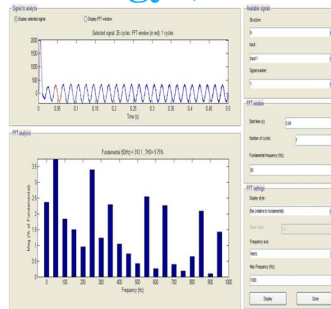


Fig. 21 Harmonic spectrum of Phase-A Source current with DSTATCOM

V. CONCLUSION

A DSTATCOM with seven levels CHB inverter is investigated. Mathematical modeling on multi-level inverters can be developed. The source voltage, load voltage, source current, load current, power factor simulation results under non-linear loads are presented. Finally Matlab/Simulink based model is developed and simulation results are presented.

REFERENCES

- [1] P.Bhagwat. and V.R.Stefanovic. "Generalized structure of a multilevel PWM Inverter." IEEE Trans. Ind. Appln, Vol.IA-19, no.6, pp. 1057-1069, Nov./Dec .. 1983.
- [2] J.Rodriguez. Jih-sheng Lai, and F Zheng peng, "Multilevel Inverters; A Survey of Topologies, Controls, and Applications," IEEE Trans. Ind. Electron., vol.49, no.4, pp.724-738, Aug.2002.
- [3] Roozbeh Naderi, and Abdolreza rahmati, "Phase-shifted carrier PWM technique for general cascaded inverters," IEEE Trans. Power.Electron., vol.23, no.3, pp. 1257-1269, May.2008.
- [4] Bhim Singh, Kamal AlHaddad & Ambrish Chandra, 1999, A Review of Active Filter for Power Quality Improvements, IEEE Trans on Industrial Electronics, 46(S), pp.960-970
- [5] Jason R. Wells, XinGengPatrick L. Chapman Philip T. Krein and Brett M. Nee, "Modulation-Based Harmonic Elimination", IEEE Transactions on power electronics, vol. 22, no. 1, pp.336-340, 2007.
- [6] J. Napoles, A. J. Watson, J. J. Padilla, J. I. Leon, L. G. Franquelo, P. W. Wheeler and M. A. Aguirre, "Selective Harmonic Mitigation Technique for Cascaded H-Bridge Converters with Non-Equal DC Link Voltages", IEEE Transactions on power electronics, pp.1-9, 2012.
- [7] John N. Chiasson, Leon M. Tolbert, Keith J. McKenzie and Zhong Du, "A Unified Approach to Solving the Harmonic Elimination Equations in Multilevel Converters", IEEE Transactions on power electronics, vol. 19, no. 2, pp.478-500, 2004.
- [8] A. Maheswari, S. Mahendran, Dr. I. Gnanambal, "Implementation of Fundamental Frequency Switching Scheme on Multi-Level Cascaded Hbridge Inverter Fed Three Phase Induction Motor Drive" Wulfenia journal, Klangfurt, Austria, Vol 19, No. 8, pp.10-24, 2012.
- [9] S.J.Kim and S.K.Sul, "A novel filter design method for suppression of high voltage gradient in voltage-fed PWM inverter," Proc. Appl. Power Electron. Conf., 1997, pp.122-127
- [10] M.M.Swamy, K.Yamada, and T.Kume, "Common mode current attenuation techniques for use with PWM drives," IEEE Trans. Power Electron., vol.16, pp.248-255, Mar. 2001
- [11] S.Ogasawara, H.Ayano, and H.Akagi, "An active circuit for cancellation of common-mode voltage generated by a PWM inverter," IEEE Trans. Power Electron. vol.13, pp.835-841, Sept.1998
- [12] S.Ogasawara, S.Zhang, and H.Akagi, "Configuration and characteristics of active canceling and compensation circuits for reducing common-mode voltage generated by voltage-source PWM inverters," Electrical engineering in Japan, vol.137, No.1, 2001, pp.57-65.



10.22214/IJRASET



45.98



IMPACT FACTOR:
7.129



IMPACT FACTOR:
7.429



INTERNATIONAL JOURNAL FOR RESEARCH

IN APPLIED SCIENCE & ENGINEERING TECHNOLOGY

Call : 08813907089  (24*7 Support on Whatsapp)